# Augmented Branch Failure Model for Energy Function Analysis in the Cascading Failure

**By**

**Honghao Zheng**

A thesis submitted in fulfillment of the

requirements for the degree of

Master of Science

(Electrical Engineering)

at the

UNIVERSITY OF WISCONSIN-MADISON

2011

**Abstract**

Failure of a single transmission line in heavily loaded electric grid can create overloads in parallel lines, subsequently inducing failure in those lines with the possibility for global, system-wide failures. For power systems engineers, the challenge is to find an efficient method for predicting "cascading" effects, and efficiently identifying scenarios that lead to large scale failure. In the literature of the last decade, progress has been made in characterizing the role of graph interconnection structure in propagation of failures in probabilistic models of electric power networks [3] [4].

Work to date has focused primarily on representations in which the state of the system is discrete, and only steady state overloads and line outages are modeled. Indeed, for computational tractability over very large numbers of scenarios, many approaches in the literature [4], [5], [6] adopt a simple transmission line failure representation based on the power flow representation; i.e. a steady state model only.

In this work, a bi-stable branch outage model for cascading failure analysis in a transient stability context is developed. Using 3 bus network and the IEEE standard 14 bus example, this thesis describes a simplified, smooth dynamic model for line outage, in which "relay" action removes a line from service when overloaded, and the effect of the line outage is then reflected in the subsequent evolution of the state trajectory.

The novel contribution here will be to demonstrate that the model can be constructed in a fashion that yields a well-defined scalar function (an "energy" function) that is guaranteed non-increasing along any state trajectory. Such energy functions have a long history in power systems analysis, and offer a useful analytic supplement to stability assessments based purely on detailed simulation data [12]. Moreover, this work conducts the first step analysis to estimate whether the system state will return to a locally stable equilibrium, or will diverge.

To allow the tractable analysis of continuous dynamics in state space models of high dimension, we will restrict attention to a specialized class of system representation, one in which energy storage associated with individual elements is closely tied to a structure of ordinary differential equations that describes the system dynamics. Key to the novel contribution here, that of representing line failures, will be the fact that the threshold failure mechanism modeled will be associated with energy storing elements. Moreover, the failure

threshold itself is expressed in terms of energy stored in the branch. While admittedly a simplification of the complex logic of transmission line protection, the model here will remove a transmission line from service when the magnitude of its current flow exceeds a user-specified threshold.

# Contents



# List of Figures

## List of Tables

# 1. Introduction

## 1.1 System Modeling in the Analysis of Cascading Failure

In the last twenty years, much research has been conducted in the analysis of cascading failure events in large-scale power systems. The premise of this work is that properly structured power system model would be valuable for analyzing the cascading failure events. Indeed, many researchers tried to construct the tractable power system model so that the risks of cascading failure could be understood and quantified.

In last decade, some progress has been made in characterizing the role of graph interconnection structure in propagation of failures in probabilistic models of electric power networks [3] [4]. The work of [3] introduced and analyzed the influence model, a tractable mathematical representation of random, dynamical interactions on networks with describing the evolution of the status at nodes according to the internal Markov Chain. The authors of [4] discuss the two types of transitions in cascading failure blackouts as the load power demand is increased, and they use the DC power flow model for simplicity.

Apart from the graph interconnection structure, the simple transmission line failure based on the DC power flow representation has also been studied to achieve the computational tractability [4] [5] [6]. The work of [5] introduced a “hidden failure” model for DC power flow, while [6] tackles the problem with a branching process model so as to estimate the propagation of load shed and also the probability distribution of load shed.

However, the work to date has focused primarily on representations in which the state of the system is discrete, and only steady state overloads and line outages are modeled. In this work, a bi-stable branch outage model for cascading failure analysis in a transient stability context is developed. Section 2.2 describes a simplified, smooth dynamic model for line outage, in which “relay” action removes a line from service when overloaded, and the effect of the line outage is then reflected in the subsequent evolution of the state trajectory. The invented branch-failure model will be devoted to the energy analysis, which is briefly reviewed in the next sub-section.

## 1.2 Lyapunov Energy Function

Through the 1970's to 1990's, much work has been conducted in analyzing the transient stability of the multi-machine power systems. For a decade, many different methods were investigated. The "energy function approach", which is one of those methods, focused on the description of the system transient energy causing the power system state to depart from the initial equilibrium state, and the power network's ability to absorb the energy so that it could reach a new post-disturbance equilibrium state [13].

In the end of 1990's, a new method for constructing Lyapunov functions for a particular class of nonlinear systems has been provided [12]. The author in [7] gave out a general, and simpler algorithm that could be applied to a given system to obtain a Lyapunov Function. The algorithm will be applied in this work to form the detailed structure of the energy function.

To enable the analytic techniques to be developed, the class of system of interest will be shown to have a special form, previously termed "quasi-gradient" in [7]:

$$\dot{x} = A\nabla\Phi(x) \tag{1-1}$$

where:

X: a state space of arbitrary dimension n,

$\Phi$: $\Re^n \rightarrow \Re$ is a (at least twice) differentiable function,

$A \in \Re^{nxn}$ is a full rank, negative semi-definite matrix.

The energy function constructed in this thesis is dependent on ALL state variables of the power system, and satisfies the hypothesis of the invariance theorem of La Salle [14]. As confirmed in the work of [7], many of the dynamic models appearing in early literature on power systems Lyapunov stability analysis can be shown to possess this special structure, with $\Phi(x)$ playing the role of the Lyapunov function.

# 2. Methodology of Branch Failure Augmented Power System Modeling

## 2.1 Power System Dynamic Model & Lyapunov Energy Function

Early work on this topic examined a nonlinear R-L-C circuit with dynamics analogous to the power system [11], work here shows that the large-scale power system could be modeled by applying the Hamiltonian-like System Model Structure. From the generator swing dynamic model, we shall have the following ordinary differential equations [15]

$$M_g \ddot{\delta}_g + D_g \dot{\delta}_g + P_G - P_M = 0 \tag{2-1}$$

$$\dot{\delta}_g = \omega_g \tag{2-2}$$

Here the $M_g = \frac{H_g}{\pi f_0}$, while $H_g$ is in the unit of "seconds" that usually ranges from 1 to 10 for typical generators, and $f_0 = 60HZ$ for the grid frequency in the United States; $D_g = \frac{2k\omega_0}{S_B^{3\phi}}$ determines the damping of the frequency oscillation; $P_G$ denotes the electrical outputs of each generator, while $P_M$ is the mechanical power that feeds the generator.

From Bergen and Hill's work [8], differential equation governing the load bus voltage angle and load bus voltage magnitude can be constructed by singular perturbation of algebraic power balance equations; that is, in the form of the multiplication of negative inverse of the time constant and the power mismatch of the injected & absorbed power at each load bus[Equation]. Though the equations simplify the real electrical structure of the large-scale power system, they still capture the major dynamic behavior in most cases [structure preserving].

$$\dot{\delta}_l = -D_l^{-1}\left(P_l^e + P_l^0\right) \tag{2-3}$$

$$\left|\dot{V}_l\right| = -\frac{1}{\varepsilon|V_l|}\left(Q_l^e + Q_l^0\right) \tag{2-4}$$

Here both $D_l$ and $\varepsilon$ may both be interpreted as time constants, usually in the range of 1/200 (former) and 4/1000 (latter). $P_l^e$ is the real power that injected into the load bus, while $P_l^0$ is the real power that absorbed by the load bus. Reactive quantities are analogously defined by $Q_l^e$, $Q_l^0$.

As discussed in the Introduction, the "quasi-gradient" form (1-1) enables the development of analytic techniques, and $\Phi(\mathbf{x})$ is an at least twice differentiable function. If we construct the negative semi-definite $\mathbf{A}$ matrix as follows:

$$\mathbf{A}=\begin{bmatrix} -\mathbf{M}_g^{-1}\mathbf{D}_g^{-1}\mathbf{M}_g^{-1} & -\mathbf{M}_g^{-1} & \mathbf{0} & \mathbf{0} \\ \mathbf{M}_g^{-1} & \mathbf{0} & \mathbf{0} & \mathbf{0} \\ \mathbf{0} & \mathbf{0} & -\mathbf{D}_l^{-1} & \mathbf{0} \\ \mathbf{0} & \mathbf{0} & \mathbf{0} & -\dfrac{1}{\varepsilon}\cdot\mathbf{I} \end{bmatrix} \tag{2-5}$$

Then we shall have

$$\begin{aligned} \frac{\partial\Phi}{\partial t} &= \left[\frac{\partial\Phi}{\partial\mathbf{x}}\right]\cdot\left[\dot{\mathbf{x}}\right] \\ &= \nabla_{\mathbf{x}}\Phi^T(\mathbf{x})\cdot\mathbf{A}\cdot\nabla_{\mathbf{x}}\Phi(\mathbf{x})\le 0 \end{aligned} \tag{2-6}$$

In other words, the Lyapunov Energy Function will be non-increasing with respect to time with negative semi-definite constant $\mathbf{A}$ matrix.

The gradient of the energy function is constructed:

$$\nabla_x\Phi(\mathbf{x})=\begin{bmatrix} \mathbf{M}_g\omega_g \\ \mathbf{P}_g^e+\mathbf{P}_g^0 \\ \mathbf{P}_l^e+\mathbf{P}_l^0 \\ \left|\mathbf{V}_l\right|^{-1}(\mathbf{Q}_l^e+\mathbf{Q}_l^0) \end{bmatrix} \tag{2-7}$$

Finally, the completed form of the energy function is deducted:

$$\Phi(\mathbf{x})=\frac{1}{2}\omega_g^T\mathbf{M}_g\omega_g+\frac{1}{2}\sum_{i=1}^{N_{bus}}\left|B_{ii}\right|\left|V_i\right|^2-\sum_{k=1}^{N_{br}}\left|B_{k,ij}\right|\left|V_{k,i}\right|\left|V_{k,j}\right|\cos\left(\delta_i-\delta_j\right)+\delta_g^T\mathbf{P}_g^0+\delta_l^T\mathbf{P}_l^0+\ln\left(\left|\mathbf{V}_l^T\right|\right)\mathbf{Q}_l^0 \tag{2-8}$$

The matrix $\mathbf{M}_g$, which is a square matrix, has each $M$ in the diagonal entry of the matrix. The $N_{bus}$ is the number of the buses in the certain power system model, and $N_{br}$ represents the number of transmission lines.

Specifically, the detailed structure of the energy function of the 3 bus system may better explain the equation (2-8):

$$\begin{aligned}\Phi_{3bus}(\mathbf{x}) = &\frac{1}{2}M_1\omega_1^2 + \frac{1}{2}M_2\omega_2^2 + \frac{1}{2}(b_1+b_2)|V_1|^2 + \frac{1}{2}(b_1+b_3)|V_2|^2 \\ &+ \frac{1}{2}(b_2+b_3)|V_3|^2 - b_1|V_1||V_2|\cos(\alpha_2) - b_2|V_1||V_3|\cos(\alpha_3) \\ &- b_3|V_2||V_3|\cos(\alpha_3-\alpha_2) + P_2^0\alpha_2 + P_3^0\alpha_3 + Q_3\ln|V_3|\end{aligned} \tag{2-9}$$

Here $\mathbf{x}_{3bus} = \begin{bmatrix}\omega_1 & \omega_2 & \alpha_2 & \alpha_3 & V_3\end{bmatrix}^T; \alpha_2 = \delta_2 - \delta_1, \alpha_3 = \delta_3 - \delta_1$

## 2.2 Branch Failure Model

To represent failure in a branch, the state space of our model will be augmented to associate an approximately binary indicator with each branch that is subject to the possibility of failure. These indicator variables will be states in a system of continuous ordinary differential equations, so their values will not truly be binary. Rather, a structure will be imposed that yields two stable equilibria to be placed in a neighborhood of 1, corresponding to the operational state of the branch, and in a neighborhood of 0, indicating a failed state. We will focus on a "one way" model: a branch that undergoes failure will have no possibility of returning to the operational state. Modifications to allow the rescolsure of the line back into service are possible, but not pursued here. We let $\gamma_k$ represent the failure indicator state for branch $k$.

The mechanism of failure that our model will represent is one in which a branch is removed from service when a specified threshold of energy storage in the branch is exceeded. This model requires that the energy function has a separable term representing branch energy storage. The goal will be to modify the energy function to introduce dependence on the branch failure states. As a representative example of the properties we seek in the threshold function, consider the scalar, real-valued function defined below:

$$\theta(\gamma) = 2[-\exp(-20\gamma) + \exp(-200\gamma) + \exp(20[\gamma - 1]) - \exp(200[\gamma - 1]) - 0.2] \tag{2-10}$$

The resulting is illustrated in figure below:

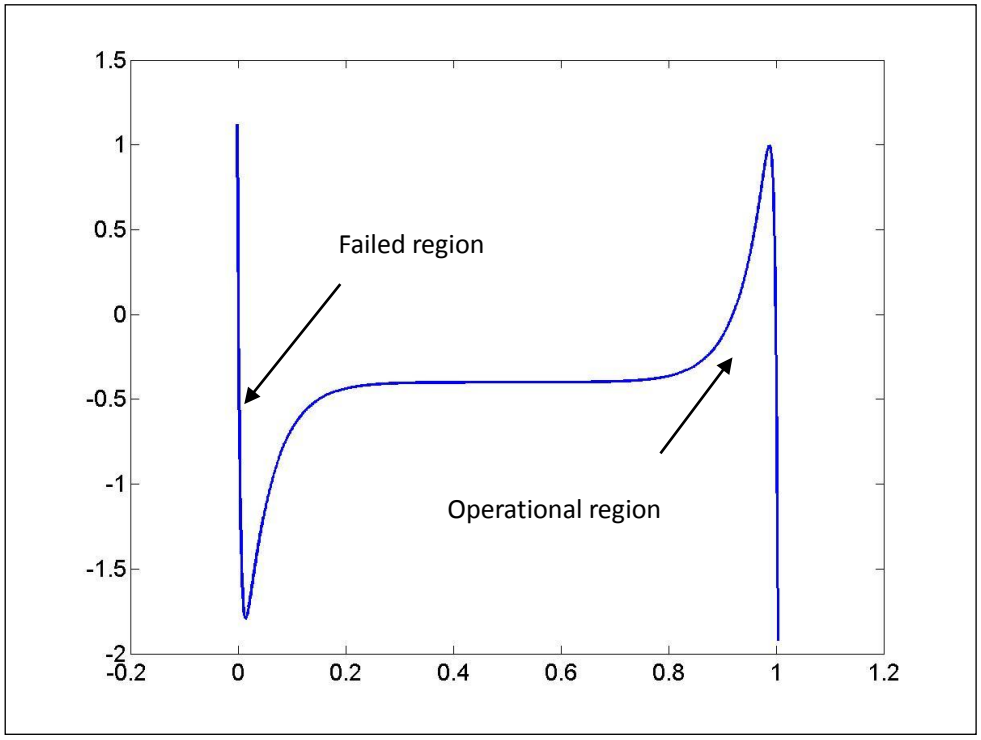


**Figure 1 Sketch of $\theta(\gamma)$ Versus $\gamma$**

The intuition behind our bi-stable branch model may be observed simply through the properties of $\theta(\gamma)$. Suppose the right hand side of an equation for $d\gamma/dt$ were composed of $\theta(\gamma)$ minus the energy storage indicator for the branch (noted as $\lambda$); e.g. $\lambda = \frac{|I_k^2|}{2b_k}$ where $I_k$ is the phasor current of branch $k$, and $b_k$ is the susceptance of branch $k$. It should be pointed out that the system is assumed lossless, which is reflected in the omission of the resistance of the transmission line.

With these dynamics driving $d\gamma/dt$, suppose $\lambda$ were to begin from an initial condition near zero, and $\gamma$ from an initial condition near 1. Suppose further that dynamics of the system are such that $\lambda$ gradually increases with time. In this scenario, $\gamma$ would maintain a stable equilibrium value in the vicinity of $\gamma = 1$ so long as $\lambda$ had a magnitude less than 1. If $\lambda$ were to exceed the threshold value of 1, $d\gamma/dt$ would become negative, tending to push $\gamma$ to values less than 1. The nature of $\theta(\gamma)$, and the fact that $\lambda$ is non-negative by construction, ensure that as soon as $\gamma$ drops below 1 by any appreciable margin, $d\gamma/dt$

becomes very strongly negative, and $\gamma$ further decreases until it is captured in a new equilibrium in the vicinity of zero. By appropriate scaling of $\theta(\gamma)$, the threshold value that initiates failure is easily parameterized in the model. Similarly, by suitable adjustment of the coefficients of the exponential terms, the slopes in the vicinity of the $\gamma = 0$ and $\gamma = 1$ critical points can be modified.

To obtain the structure of state equations that allows the energy function $\Phi(\mathbf{x})$ to serve as a global Lyapunov function in our augmented model, it is a sign reversed integral of $\theta(\gamma)$ that must be incorporated. Hence, our interest focuses on the integrated function:

$$\Theta(\gamma) = \int_{1}^{\gamma} -\theta(\eta) d\eta \tag{2-11}$$

For the representative $\theta(\gamma)$ illustrated in fig. 1, the resulting $\Theta(\gamma)$ is shown below in fig. The graph of $\Theta(\gamma)$ makes clear the qualitative properties we have obtained: local minima about 1 and 0, with a potential barrier blocking the transition from 1 to 0, the height of which is determined by the failure threshold.

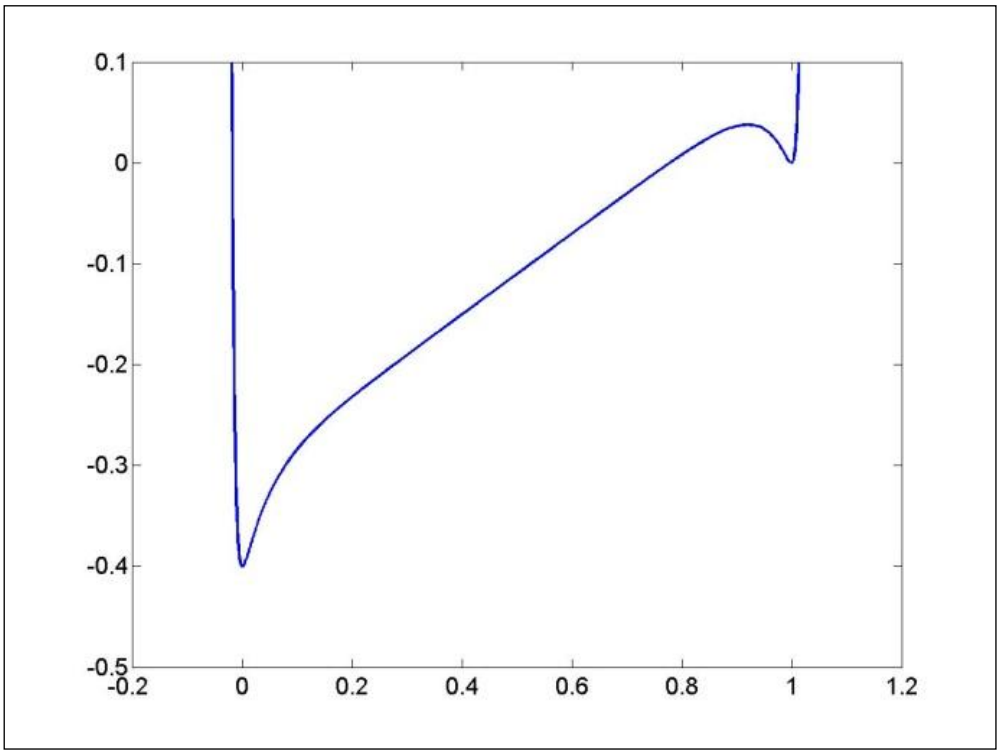


**Figure 2 Sketch of $\Theta(\gamma)$ Versus $\gamma$**

With the equation (2-9) of the original model, we shall have the augmented power system differential equation model with the bi-stable branch failure model, so as the new form of the energy function $\Phi(\mathbf{x})$.

## 2.3 Addition of Branch Failure Dynamics to the Model

### 2.3.1 Addition to the Simple 3 Bus Model

As motivated earlier, with each branch of the network, an (ideally) binary failure indicator variable, $\gamma_k$, will be associated with the property that:

$$\gamma_k = \begin{cases} 1 \text{ when branch k is operational} \\ 0 \text{ when branch k is failed} \end{cases}$$

The replacement of $b_k$ by $\gamma_k \cdot b_k$ is necessary in this augmented model. Still, the simplest 3 bus system continues to act as an example and the modified energy function is denoted as $\Phi_{3bus\_m}(\omega_1, \omega_2, \alpha_2, \alpha_3, V_3, \gamma_1, \gamma_2, \gamma_3)$.

The element failure is to be triggered by a branch current $|\mathrm{I}|$ exceeding a specified threshold. The goal is to modify the energy function $\Phi_{3bus\_m}$ to introduce dependence on the branch failure states. In particular, one has to seek a $\Phi_{3bus\_m}$ with the property that $\partial\Phi_{3bus\_m} / \partial\gamma$ recovers a term suitable for "driving" the time derivative of $\gamma$.

Let us consider the link between $\partial\Phi_{3bus\_m} / \partial\gamma$ and the branch current magnitude $|\mathrm{I}|$. The complex current flow on line 1 is

$$\vec{I}_1 = (jb_1)(\vec{V}_1 - \vec{V}_2) \tag{2-12}$$

Then

$$\left|\vec{I}_1\right|^2 = \vec{I}_1 \vec{I}_1^* \tag{2-13}$$

$$\begin{aligned} \left|\vec{I}_1\right|^2 &= b_1^2(\left|V_1^0\right|^2 - \vec{V}_1\vec{V}_2^* - \vec{V}_2\vec{V}_1^* + \left|V_2^0\right|^2) \\ \left|\vec{I}_1\right|^2 &= b_1^2(\left|V_1^0\right|^2 - 2\left|V_1^0\right|\left|V_2^0\right|\cos(\alpha_2) + \left|V_2^0\right|^2) \\ \left|\vec{I}_1\right|^2 &= 2b_1 \frac{\partial\Phi_{3bus\_m}}{\partial\gamma_1} \end{aligned} \tag{2-14}$$

Similarly

$$\left|\vec{I}_2\right|^2 = 2b_2 \frac{\partial\Phi_{3bus\_m}}{\partial\gamma_2}, \ \left|\vec{I}_3\right|^2 = 2b_3 \frac{\partial\Phi_{3bus\_m}}{\partial\gamma_3} \tag{2-15}$$

Now, suppose we modify $\Phi_{3bus}$ further, to add a $\gamma_k$ dependent term for each branch; in the case of our simple 3 bus example, this would take the form:

$$\Phi_{3bus\_m} = \Phi_{3bus} + \sum_{k=1}^{3} W_k \Theta(\gamma_k) \tag{2-16}$$

In the above expression, $W_k$ represents the energy threshold of the corresponding transmission line.

Then

$$\frac{\partial \Phi_{3bus\_m}}{\partial \gamma_k} = \frac{1}{2b_k}\left|\vec{I}_k\right|^2 - W_k \theta(\gamma_k) \tag{2-17}$$

With this definition, we may construct a state equation for $\gamma_k$ as:

$$\dot{\gamma}_k = \frac{-1}{\tau_k}\frac{\partial \Phi_{3bus\_m}}{\partial \gamma_k} \tag{2-18}$$

(With $\tau_k$ a small time constant governing the speed of the failure transition)

Therefore, our 3 bus example system would now have 8 states, with the state equations taking the form:

$$\begin{aligned} &\mathbf{X}_{3bus\_m} = \begin{bmatrix} \omega_1 & \omega_2 & \alpha_2 & \alpha_3 & V_3 & \gamma_1 & \gamma_2 & \gamma_3 \end{bmatrix}^T \\ &\alpha_2 = \delta_2 - \delta_1, \alpha_3 = \delta_3 - \delta_1 \end{aligned} \tag{2-19}$$

The resulting gradient of energy function respect to this full set of states is given below:

$$\nabla_{\vec{x}} \Phi_{3bus\_m}(\mathbf{x}_{3bus\_m}) = \begin{bmatrix} M_1\omega_1 \\ M_2\omega_2 \\ p_1(\alpha_2) + p_2(\alpha_2 - \alpha_3) + P_2^0 \\ p_2(\alpha_3 - \alpha_2) + p_3(\alpha_3) + P_3^0 \\ |V_3|^{-1}(g_3 + Q_3^0) \\ \dfrac{|I_1|^2}{2\gamma_1 b_1} - W_1\theta(\gamma_1) \\ \dfrac{|I_2|^2}{2\gamma_2 b_2} - W_2\theta(\gamma_2) \\ \dfrac{|I_3|^2}{2\gamma_3 b_3} - W_3\theta(\gamma_3) \end{bmatrix} \tag{2-20}$$

As a notice

$$p_k(\alpha) = (-b_k)\gamma_k |V_i||V_j| \sin(\alpha) \tag{2-21}$$

and

$$g_3 = ((-b_2)\gamma_2 + (-b_3)\gamma_3)|V_3|^2 - (-b_2)\gamma_2 |V_3||V_1| \cos(\alpha_3) - (-b_3)\gamma_3 |V_3||V_2| \cos(\alpha_3 - \alpha_2) \tag{2-22}$$

$$\mathbf{A}_{3bus\_m} = \begin{bmatrix} \mathbf{A}_{3bus} & \mathbf{0} \\ \mathbf{0} & -\tau^{-1} * \mathbf{I} \end{bmatrix} \tag{2-23}$$

Thus we have $\dot{\mathbf{x}} = \mathbf{A}_{3bus\_m} \nabla_x \Phi(\mathbf{x}_{3bus\_m})$ for the 3 bus system.

### 2.3.2 Generalized Model

Similarly, we could integrate the branch failure model into the n (n>3) bus system as the following:

Analogous steps yield the augmented state equations to include branch failure in the n bus system.

$$\tilde{\mathbf{A}} = \begin{bmatrix} \mathbf{A} & \mathbf{0} \\ \mathbf{0} & -\frac{1}{\tau} * \mathbf{I} \end{bmatrix} \tag{2-24}$$

as a notice $\dot{\mathbf{x}} = \begin{bmatrix} \dot{\omega}_g \\ \dot{\delta}_g \\ \dot{\delta}_l \\ |\dot{V}_l| \\ \dot{\gamma}_k \end{bmatrix}$.

Also here the time constant $\tau$, like $D_l$ and $\varepsilon$ discussed in Section 2.1, is chosen to be 4/4000 so that the time span of line failure will close to the real situation.

Then we shall have

$$\nabla_x \Phi(\mathbf{x}) = \begin{bmatrix} \mathbf{M}_g \omega_g \\ \mathbf{P}_g^e + \mathbf{P}_g^0 \\ \mathbf{P}_l^e + \mathbf{P}_l^0 \\ \frac{1}{|\mathbf{V}_l|}(\mathbf{Q}_g^e + \mathbf{Q}_g^0) \\ \frac{1}{2\gamma_k b_k}\left|\vec{\mathbf{I}}_k\right|^2 - \mathbf{W}_k \theta(\gamma_k) \end{bmatrix} \tag{2-25}$$

Finally, the expansion of the original energy function will be constructed as follows:

$$\begin{aligned} \Phi(\mathbf{x}) = {} & \frac{1}{2}\omega_g^T \mathbf{M}_g \omega_g + \frac{1}{2}\sum_{i=1}^{N_{bus}} \left|B_{ii}(\gamma)\right| \left|V_i\right|^2 - \sum_{k=1}^{N_{br}} \left|B_{k,ij}(\gamma)\right| \left|V_{k,i}\right| \left|V_{k,j}\right| \cos\left(\delta_i - \delta_j\right) \\ & + \delta_g^T \mathbf{P}_g^0 + \delta_l^T \mathbf{P}_l^0 + \ln\left(\left|\mathbf{V}_l^T\right|\right)\mathbf{Q}_l^0 + \sum_{k=1}^{N_{br}} W_k \Theta\left(\gamma_k\right) \end{aligned} \tag{2-26}$$

# 3 Simulation Result & Energy Analysis

## 3.1 Sufficient Condition for Ensuring Recovery to a Stable Operating Point

Now, consider an analyst having in hand simulation data over a time interval out through the time at which one branch has failed. The challenge is to try to predict if the system converges back to a stable equilibrium with all other lines in service, or if the system moves away from this desirable operating region by experiencing further branch failures. The ultimate goal of the work here will be to use properties of the energy function to establish sufficient conditions for the system state to be captured in an attractive region about an operable (if partially degraded) network configuration.

Since $\Phi(X(t))$ is non-increasing along trajectories of the system, one can claim that a sufficient condition that guarantees convergence to $X^s$ is : $X^0 \in$ component of $\{X| \Phi(X)<\Phi(X^{u,min}) \}$ containing $X^s$.

So, a practical test to guarantee that $X^0$ converge to $X^s$ might be constructed as :

1) Check that $\Phi(X^0)<\Phi(X^{u,min})$

2) Ensure that there exists a one dimensional path connecting $X^0$ to $X^s$ such that $\Phi$ is non-increasing along this path.

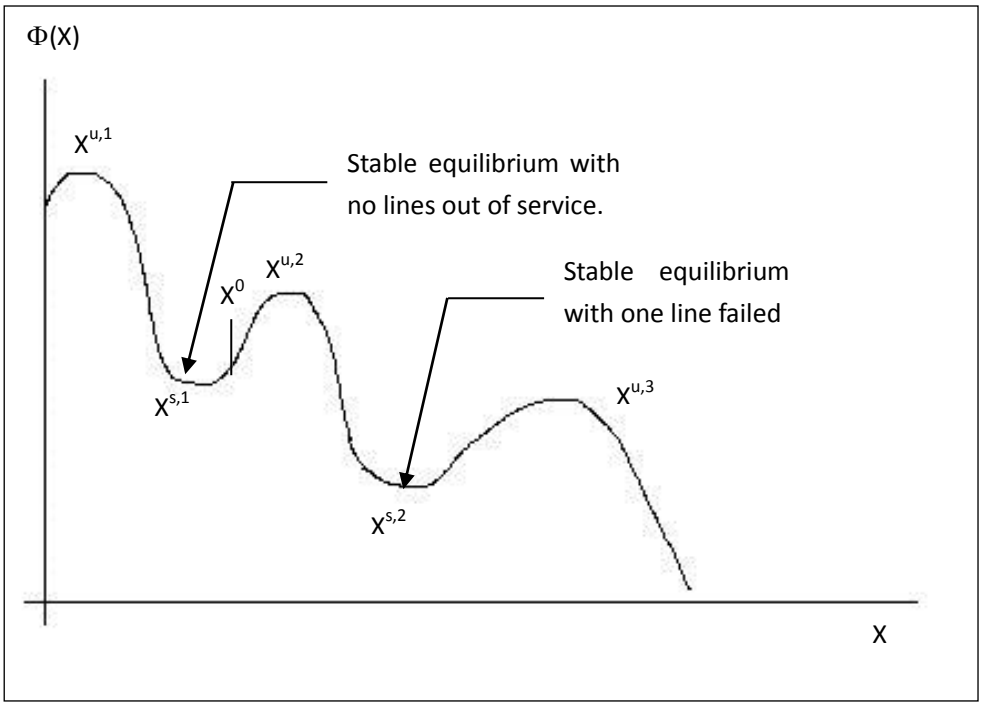


**Figure 3 Conceptual Plot for Φ(x) versus x**

Note: The path connecting $X^0$ to $X^s$ may be found by following the direction given by an eigenvector of $\frac{\partial^2 \Phi}{\partial^2 X}$. Only an eigenvector related to a negative eigenvalue ensures that Φ is non-increasing along this path.

## 3.2 One Line Failure Study

### 3.2.1 Line Failure Simulation

The single line failure simulation described in this section aims to demonstrate the feasibility of the branch failure model, which followed by the energy contour plot analysis. The figure below displays the detailed one-line diagram of the 3 bus system, followed by the initial state and corresponding disturbance input condition. Since the system is lossless, the resistance of each transmission line is neglected and therefore the susceptance dominates the dynamic behavior of the system.

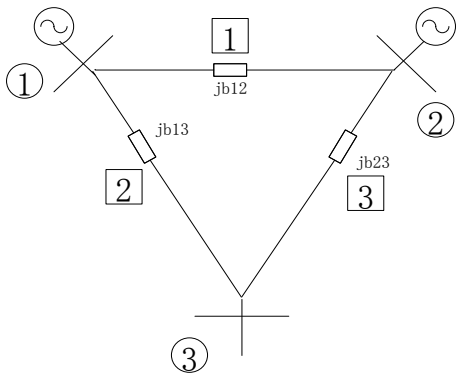


**Figure 4 Power System 3 Bus Case**

Slack Bus: Bus 1; Gen Bus: Bus 2; Load Bus: Bus 3

Initial Condition:

$$M_1 = 0.052, M_2 = 0.0531, b_1 = b_2 = b_3 = 10, b_1 = b_{12}, b_2 = b_{13}, b_3 = b_{23}$$

$$P_2^0 = -2.0, P_3^0 = 3.0 + j0.1, D_l = 0.005, D_g = 0.05$$

$$V_1 = 1.06e^{j0}, V_2 = 1.01e^{j\frac{1.9296}{\pi}}, V_3 = 1.0194e^{j\frac{-7.2328}{\pi}}$$

Step Input (at t = 0s): $P_2^0 = -2.0 \rightarrow P_2^0 = -3.0$ (All in Per Unit)

In the beginning, the system works at the steady state. The load absorbs 3 units of active power and 0.1 units of reactive power, while the generator on bus 2 injects 2 units of active power to the system. Because the bus 1 is treated as an infinite bus, it will provide the remaining part of the power. Then at t=0s, the generator on bus 2 pumps the injection of active power from 2 to 3 units, which results in the increasing current flow on branch 3. When

the magnitude of the current exceeds the threshold setting for branch 3, the gamma function operates and the line fails.

The plots below illustrate the time behavior of $\gamma_3(t)$, as well as the power flow through branch 3:

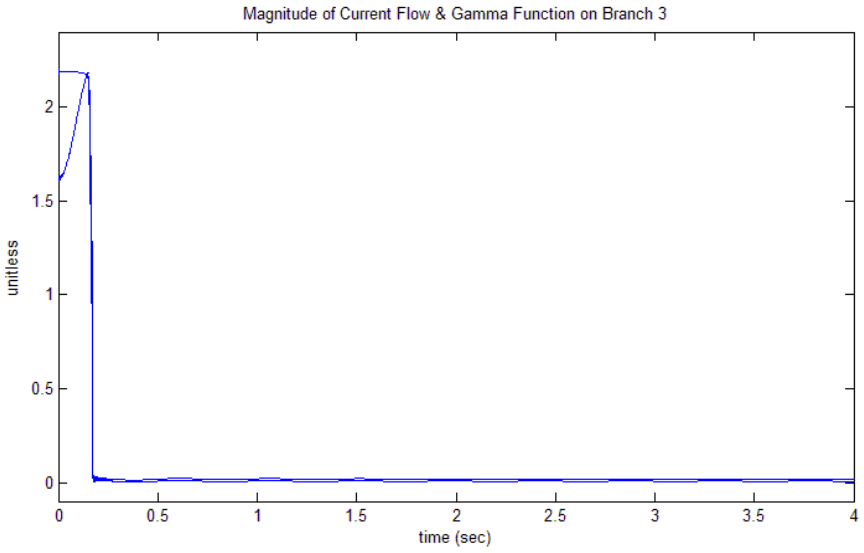


**Figure 5 Magnitude of Current Flow on Branch 3 with $\gamma_3(t)$ Curve**

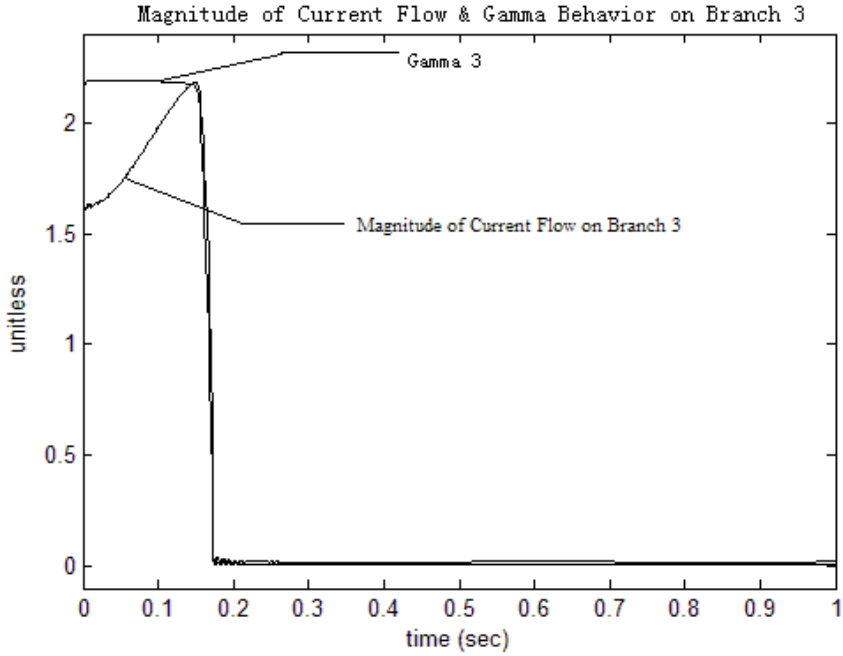


**Figure 6 Magnitude of Current Flow on Branch 3 with $\gamma_3(t)$ Curve (Detail from 0s to 1s)**

These two figures suggest that the gamma function's representation for the behavior of the relay's on/off operation captures the desired qualitative behavior, because of short response time and rapid decreasing magnitude.

### 3.2.2 Energy Contour Plot (Two Degrees of Freedom)

The energy function $\Phi_{3bus\_m}(\mathbf{x}(t))$ could be expressed as below:

$$\begin{aligned}
&\Phi_{3bus_m}(\omega_1,\omega_2,\alpha_2,\alpha_3,|V_3|,\gamma_1,\gamma_2,\gamma_3) = \frac{1}{2}M_1\omega_1^2 + \frac{1}{2}M_2\omega_2^2 \\
&+\frac{1}{2}(\gamma_2 b_2 + \gamma_3 b_3)|V_3|^2 + \frac{1}{2}(\gamma_1 b_1 + \gamma_2 b_2)|V_1^o|^2 + \frac{1}{2}(\gamma_1 b_1 + \gamma_3 b_3)|V_2^o|^2 \\
&-\gamma_2 b_2 |V_3||V_1^o|\cos(\alpha_3) - \gamma_3 b_3 |V_3||V_2^o|\cos(\alpha_3 - \alpha_2) \\
&-\gamma_1 b_1 |V_1^o||V_2^o|\cos(\alpha_2) + P_2^o\alpha_2 + P_3^o\alpha_3 + Q_3 \log V_3 + \sum_{k=1}^{3}\Theta(\gamma_k)W_k
\end{aligned} \tag{3-1}$$

Now we examine trajectories for the failure of line 3, plotting the behavior of the energy function with respect to time:

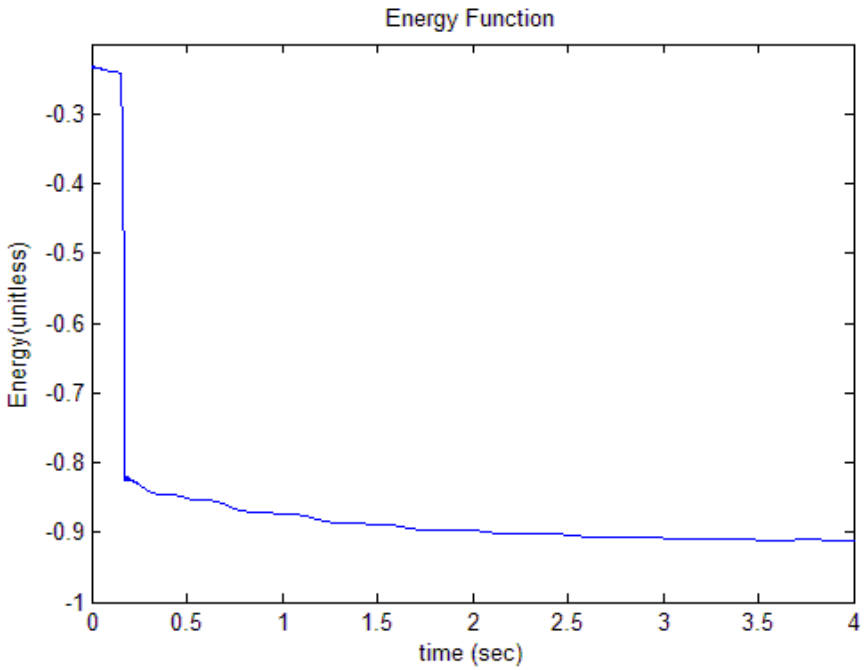


**Figure 7 Decay of Energy versus Time**

The graph above displays that the value of energy function stays nearly constant when the 3 bus system operates at nominal condition. When the failure of line 3 is triggered around 0.1s, which results in the rapid decreasing of the value of $\Phi(\mathbf{x}(t))$. After about 3s, the system gradually reach another equilibria and becomes stable again, then the value of the $\Phi(\mathbf{x}(t))$ decays more slowly.

To illustrate the idea graphically in a contour plot, an examination of the behavior with respect to two degrees of freedom has been chosen. Judicious selection of the two degrees of freedom is important, and in real power system, the more rigorous conditions for the higher dimensional state space should be considered.

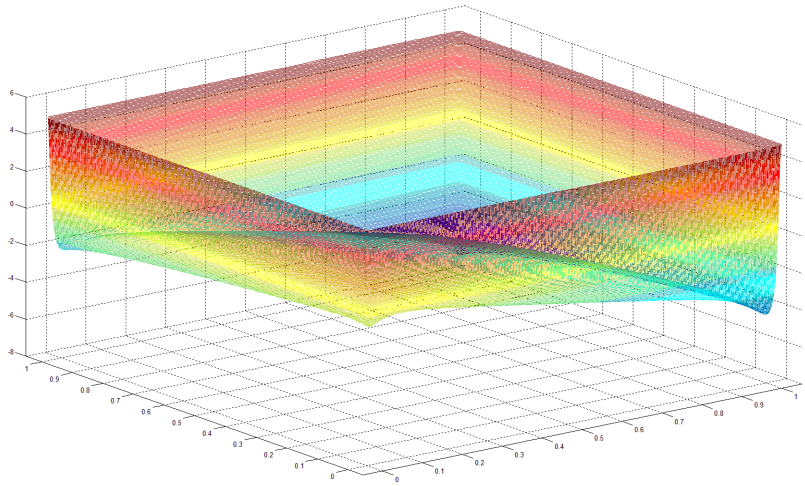

**Figure 8 3-D plot of the Energy Function versus State Variables**

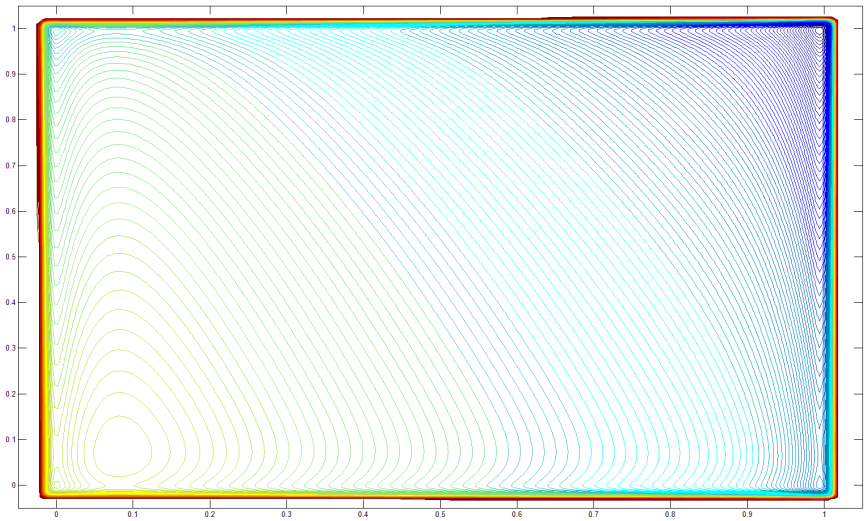

**Figure 9 2-D plot of the Energy Function versus State Variables**

## 3.3 Cascade Failure Study (Multiple Lines Fails)

Since the cascading failure events usually occur in the large scale power systems, it would be useful if we could visualize such a scenario. This sub-section treats the standard IEEE 14 BUS System as the testing model. Still, the condition of the lossless transmission line holds. The Fig.10 shows the detailed one line diagram of the standard IEEE 14 Bus System.

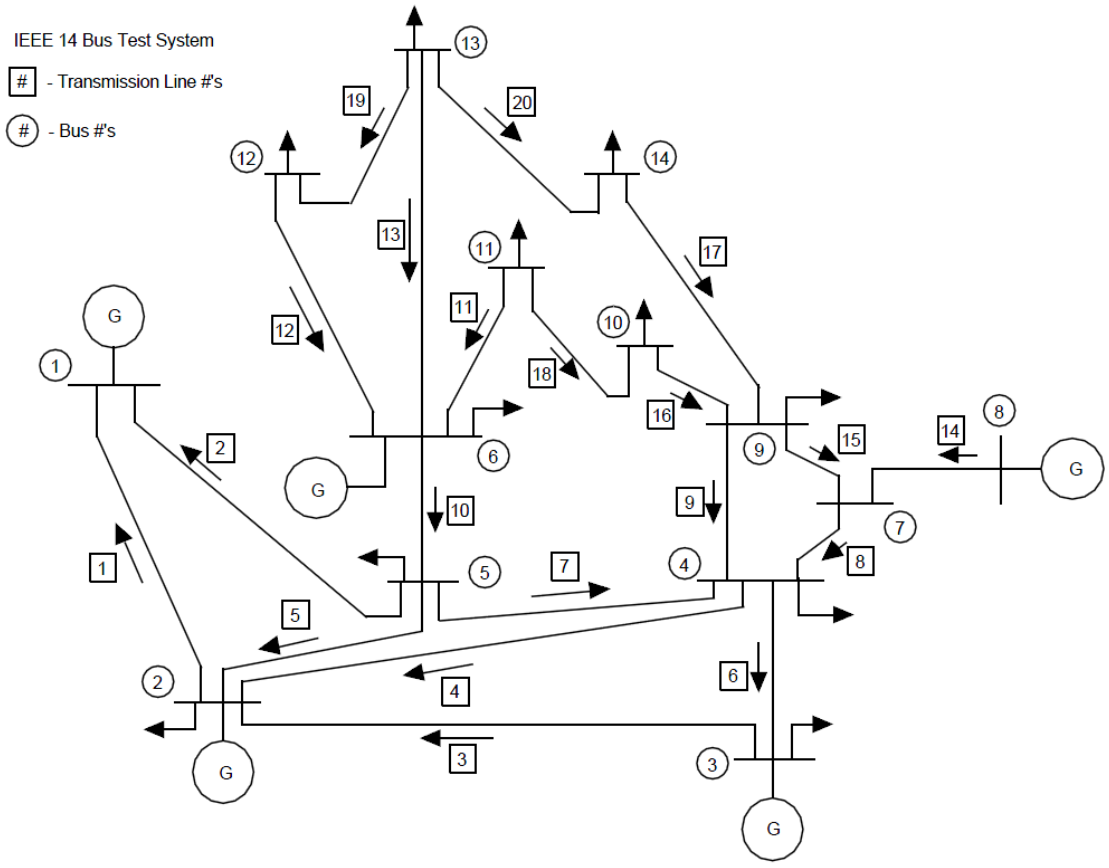


**Figure 10 One Line Diagram of the IEEE 14 Bus System**

### 3.3.1 Cascade Failure Simulation

The simulation starts with the initial condition as following:

**Table 1 Initial Condition for IEEE 14 Bus System**

| Bus No. | Voltage Magnitude | Angle (Degrees) | Real Power Injection | Reactive Power Injection |
|---|---|---|---|---|
| 1 | 1.0600 | 0 | 0.2003 | 0.3023 |
| 2 | 1.0450 | -0.3089 | 0.1001 | -0.0339 |
| 3 | 1.0100 | 0.0096 | 0.1702 | -0.3156 |
| 4 | 1.0391 | -1.5240 | -0.4005 | 0.0401 |
| 5 | 1.0457 | -1.3352 | -0.0701 | -0.0100 |
| 6 | 1.0700 | -2.1553 | 1.0013 | 0.6887 |
| 7 | 1.0372 | 0.1980 | 0 | 0 |
| 8 | 1.0900 | 8.2801 | 0.9012 | 0.3899 |
| 9 | 1.0134 | -4.2891 | -0.3505 | -0.1502 |
| 10 | 1.0127 | -5.5465 | -0.2003 | -0.0601 |
| 11 | 1.0254 | -5.9588 | -0.3304 | -0.1202 |
| 12 | 1.0319 | -7.2350 | -0.3605 | -0.1202 |
| 13 | 1.0361 | -6.0343 | -0.2804 | -0.0801 |
| 14 | 0.9922 | -9.0820 | -0.3805 | -0.1502 |

From Equation (2-15) and (2-17), we have

$$W_k = \frac{\left|\vec{I}_{k\max}\right|^2}{2b_k}, b_k > 0, b_k \in \Re \tag{3-2}$$

Before the disturbed injection, an assumption has been made that Line 2, 12, 15 & 17 are all so-called “weak lines”, because of which could not afford heavy load flow. In addition, the detailed energy threshold of each line is set to be

$W_2 = 0.02, W_{12} = 0.02, W_{15} = 0.04, W_{17} = 0.0125, W_{others} = 3.0$.

Disturbance Input: when t = 1s, the load demand of the active power at bus 5 increases from 0.07 to 0.77 per unit.

From Fig.13, apparently the increment of the load at bus 5 directly increases the power flow on line 2, which connects bus 5 and bus 1. The ascending of the power flow on line 2 exceeds the energy threshold after about a quarter second and then relay acts to trip the line 2 off (Fig.12). The loss of the line 2 causes a fluctuation of the load flow in the system. The direct influence is that the current flow oscillation begins in line 17, which reaches its threshold at the second peak and causes another line failure. The loss of two lines results in another power flow swing in the system, and sharply increases the magnitude of the current go through the line 12. According to the low energy threshold pre-defined, the third line trips. The system finally goes stable after the consecutive failure of the 3 lines out of 20 lines (Fig.11) in total.

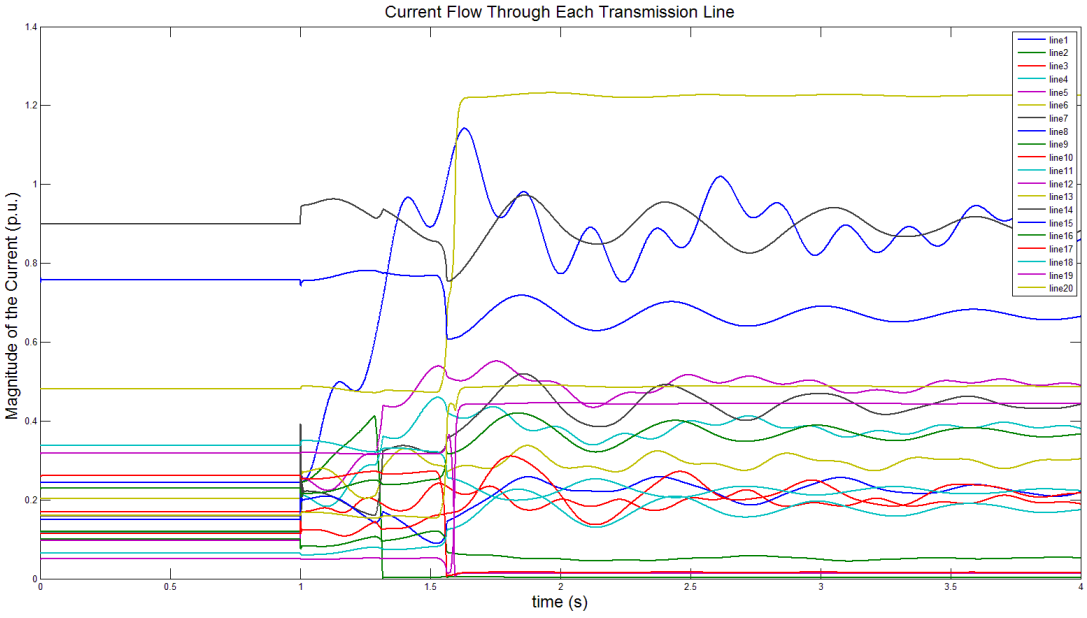


**Figure 11 Current Flow Through Each Transmission Line**

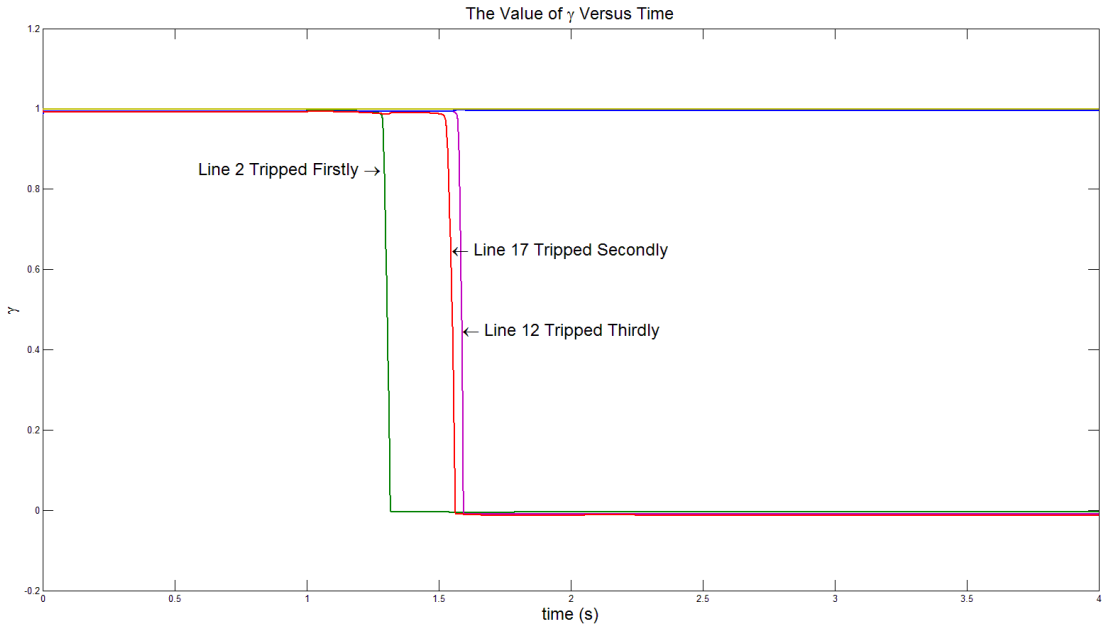


**Figure 12 The Value of $\gamma$ Versus Time**

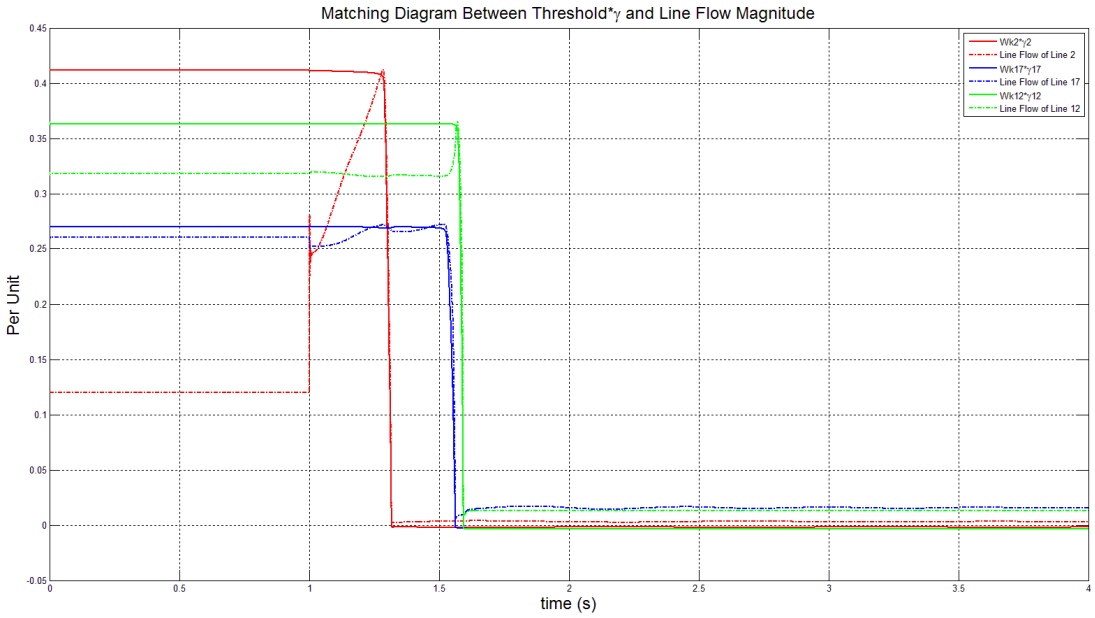


**Figure 13 Matching Diagram Between $\left|\vec{I}_{k,\max}\right|\cdot\gamma_k$ and Line Flow Magnitude $\left|\vec{I}_k\right|$ Versus Time**

### 3.3.2 Energy Analysis

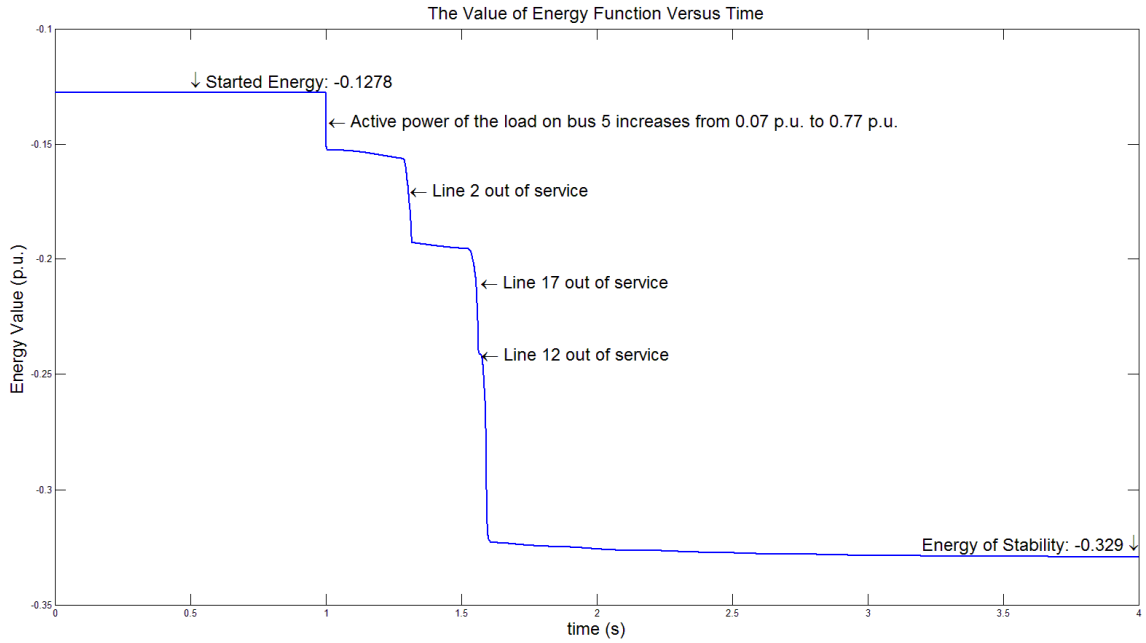


**Figure 14 The Value of Energy Function $\Phi(\mathbf{x})$ Versus Time**

The Fig.14 as shown above illustrates the detailed behavior of the energy function with respect to the cascading failure events of the IEEE 14 Bus System. As the load increases, an obvious instant drop displays onto the energy function. After about 15 cycles, the line 2 is tripped out, which results in another descend of the energy. Similarly, the line 17 goes out after about 12 cycles and so does line 12 after 1 cycle. The value of energy experiences another two drops and finally converges to equilibrium after 3.5 seconds.

Now we could apply the sufficient condition presented in the Section 3.1 to the real time simulation. To begin with, suppose all the possible unstable equilibriuas have been calculated. This work has focused on two types of UEPs: one is equilibrium that only one load bus voltage is around 0.1 [13] (the so-called "the UEP of voltage collapse point"); the other is determined by the function $\theta(\gamma)$, choose $\gamma \approx 0.92$ so that the line will fail if the value of $\gamma$ is pushed to the negative side. The energy of all the possible UEPs is displayed below:

NOTICE: The "Energy Difference" denotes the difference between steady state energy with all lines in service and the corresponding energy of unstable equilibriums.

The calculation of the energy difference of the UEPs concerning of certain lines is straightforward:

$$W_{energy\_diff} = W_k \Theta(\gamma_k), \gamma_k \approx 0.9218 \tag{3-3}$$

As indicated in the beginning of this sub-section, we have

$$W_2 = 0.02, W_{12} = 0.02, W_{15} = 0.04, W_{17} = 0.0125, W_{others} = 3.0$$

**Table 2 Possible UEPs for the IEEE 14 Bus System with Augmented Line Failure Model**

| Bus No. (V in p.u.) | Energy Difference | Line No. | Energy Difference |
|---|---|---|---|
| Bus 4 | 11.3050 | 1 | 0.1 |
| Bus 5 | 11.7424 | 2 | 0.1*0.02/3 |
| Bus 7 (N/A) | N/A | 3 | 0.1 |
| Bus 9 (N/A) | N/A | 4 | 0.1 |
| Bus 10 | 2.6346 | 5 | 0.1 |
| Bus 11 | 2.5101 | 6 | 0.1 |
| Bus 12 | 1.8679 | 7 | 0.1 |
| Bus 13 | N/A | 8 | 0.1 |
| Bus 14 | 1.1799 | 9 | 0.1 |
| Bus 11 & 14 | 3.0479 | 10 | 0.1 |
| Bus 12 & 14 | 2.6402 | 11 | 0.1 |
| | | 12 | 0.1*0.02/3 |
| | | 13 | 0.1 |
| | | 15 | 0.1*0.04/3 |
| | | 16 | 0.1 |
| | | 17 | 0.1*0.0125/3 |
| | | 18 | 0.1 |
| | | 19 | 0.1 |
| | | 20 | 0.1 |

The table above indicates that the starting energy of the disturbance (around -0.155, which is even less than the initial SEP) is less than all the calculated UEPs' energy, which satisfies the condition 1).

The next step is to find all the possible SEPs that the system could converge to, and ensure that there exists one dimensional path connecting $X^0$ to $X^s$ such that $\Phi$ is non-increasing along this path. In practical, we have to calculate all the possible SEPs' states and testing them one by one.

Here only one analytical example with plot will be given out. Suppose the system may converge to the steady state that without the line 2,7,12 and 17 or the steady state without the line 2, 12 and 17. Below are the two graphs that picks one degree of freedom, which corresponds to the vector of $\mathbf{x}^{direct} = \mathbf{x}^{disturbed} - \mathbf{x}^{stable}$. The graphs are plotted based on the equation

$$\mathbf{x}^{disturbed} = \alpha \mathbf{x}^{direct} + \mathbf{x}^{stable}, \alpha \in [0,1] \tag{3-4}$$

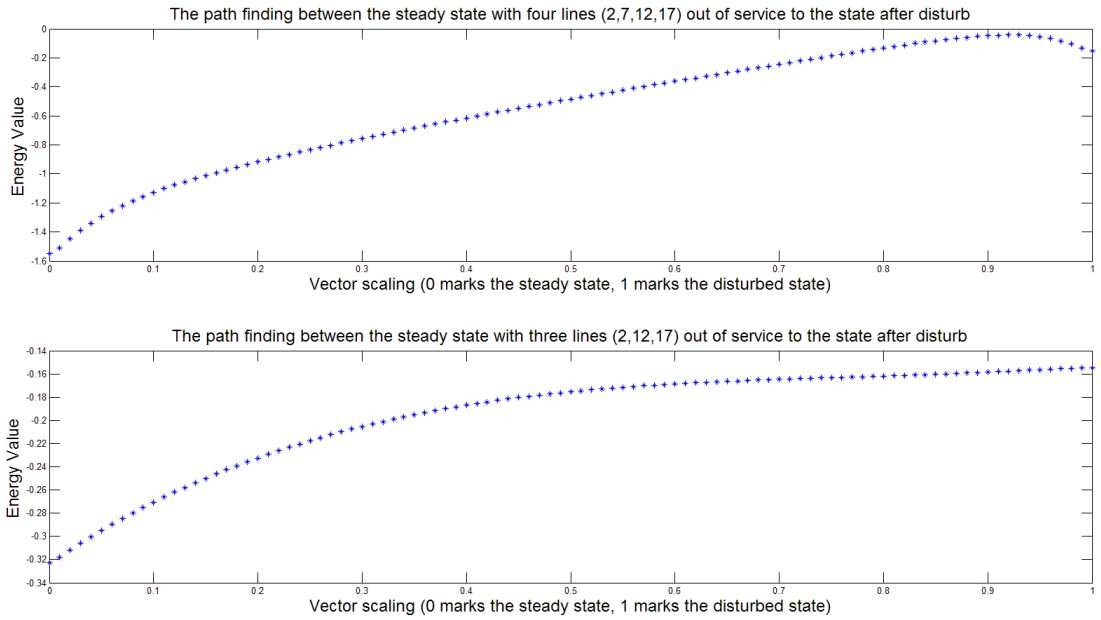


**Figure 15 The Path Finding From Different Stable Equilibrium to the Same Disturbed State**

The graph above clearly shows that the second situation (i.e. 3 lines out of service) satisfies the condition 2). The analysis only compares the two situations, but it is also true for

all the other possible SEPs, which is, the other possible SEPs will not satisfy the condition 2). Hence the system state will surely converge back to the steady state that 3 lines out of service.

Therefore, in the case discussed above, when the initial disturbed states satisfies the sufficient condition for ensuring the recovery to the operating point, no more action is needed and the system will gradually stop oscillating and operate at some degraded conditions again.

# 4. Future Work and Conclusion

## 4.1 Future Work

There are still some aspects that could be investigated in the future work. The most important one will be to efficiently identify unstable equilibrias on the boundary of regions of attraction about a stable equilibrium of interest. Preliminary investigations suggest that the unstable equilibria of interest for the bi-stable branch failure model will have interesting properties [11], quite different (and likely computationally much more tractable) from the unstable equilibria in traditional power system Lyapunov stability studies.

Another aspect mainly deals with the expansion of the existing model to include the generator tripping. When the frequency variation of a certain generator exceeds the set absolute limit, it will disconnect itself and quit the operation status. This idea has already been successfully performed in the simple 3 bus system, and will be applied to large-scale power system simulation. With the inclusion of the line failure and generator tripping, the behavior of the energy function could be better studied.

The last topic that should be undertaken seriously is how to improve the efficiency of calculating the states of all the possible UEPs and SEPs. Till now, not many effective methods have been explored, and most of the existing methods are computational costly. This barrier impedes the expansion of the method this thesis discussed to further application in large-scale power systems.

## 4.2 Conclusion

This work has stated a method that could simplify the transmission relay into the bi-stable transmission branch failure model. Moreover, the detailed model and the Lyapunov equation of large scale power system are given, and the energy function analysis is also presented. To some extent, this work step further in the state of the art of analytic cascading failure analysis.

Building on long-standing literature on energy-based stability analysis for power systems, this work has developed a new dynamic model that augments the structure preserving representation of [2], introducing a new class of dynamics that approximates protective relay action on transmission lines. This bi-stable branch failure model follows the conceptual development of [11], in which an R-L-C circuit model with branch failures was derived. It exploits the characteristics of an energy function in which a separate term is associated with each element, and the dynamics of branch failure are triggered by energy storage in the branch exceeding a specified threshold. The power system energy function exhibits this same property, and this paper demonstrated that the failure threshold in terms of branch energy can be re-expressed as a threshold in terms of the magnitude of rms branch current; i.e., the model triggers removal of a transmission line from service when the magnitude of its current is too large. While this representation oversimplifies the complex logic of transmission system protective relays, it represents a step forward in the state of the art for analytic cascading failure analysis, which to date has primarily addressed only steady state representations of line overload in DC power flow models.

As in historic developments in energy functions for power systems, it is envisioned that the energy function and dynamic model developed here will serve as a supplement to more detailed time domain simulation of specific failure scenarios and trajectories. Among the applications planned for this work are visualization tools that project system trajectories onto a two dimensional subspace or manifold, and plot energy function contours relative to the two degrees of freedom motion (for example, one might examine state trajectories in two dimensional subspace spanned by the eigenvectors of a dominant swing mode). The plots of Fig.8 and Fig.9 provide initial illustration of how the energy function contours might be

displayed and interpreted over the range of a two-degree of freedom subspace.

The development of a system model and associated energy function represents only a first step in useful application of these energy-based cascading failure analysis tools. In many ways, the most useful application of energy method lies in estimating domains of attraction about (locally) stable equilibria. The novel feature in this model is that multiple stable equilibria can be associated with partially degraded system configurations, in which some subset of lines has been removed from service, but in which the system could plausibly recover to an operable condition.

Ultimately, although "the sufficient condition to guarantee stable" has some certain limitations, it is hoped that these techniques will add to the set of tools available for predicting and preventing cascading failure in large scale power systems.

# References


[1] Koenyi Bae and J.S. Thorp, “An importance sampling application : 179 bus WSCC system under voltage based hidden failures and relay misoperations”, Proceedings of the Thirty-First Hawaii International Conference on System Sciences, Volume 3, pp 39-46, 1998.

[2] N. Narasimhamurthi and M. R. Musavi, "A general energy function for transient stability analysis of power system," IEEE Trans. on Circuits and Systems Vol. CAS-31, pp.637-645, 1984.

[3] C. Asavathiratham, “The Influence Model : A Tractable Representation for the Dynamics of Networked Markov Chains”, Ph.D. thesis, Dept. of Electrical Engineering and Computer Science, Massachusetts Institute of Technology, Cambridge, MA, October 2000.

[4] B.A. Carreras, V.E. Lynch, I. Dobson, “Critical points and transitions in an electric power transmission model for cascading failure blackouts”, Chaos, vol.12, no.4, p.985-94, December 2002.

[5] J. Chen, J. S. Thorp, "A reliability study of transmission system protection via a hidden failure DC load flow model," IEE Fifth International Conference on Power System Management and Control, pp 384–389, 2002.

[6] J. Kim, I. Dobson, "Propagation of load shed in cascading line outages simulated by OPA," Proc. of COMPENG 2010: Complexity in Engineering, Rome Italy, February 2010.

[7] C.L. DeMarco, “A New method of Constructing Lyapunov Functions for Power Systems,” Proc. IEEE Int. Symp. On Circuits and Sys., pp. 905-908, Helsinki, Finland, 1988.

[8] A.R. Bergen, D.J. Hill, “A Structure Preserving Model for Power System Stability Analysis”, IEEE Transactions on Power Apparatus and Systems, vol. PAS-100, no 1, pp 25-35, January 1981.

[9] R.A. DeCarlo, M.S. Branicky, S. Petterson and B. Lennartson, “Perspectives and Results on the Stability and Stabilizability of Hybrid Systems”, Proc. of the IEEE, vol. 88, no. 8, pp 1069-1082, July 2000.

[10] P. Varaiya, F. Wu, R-l Chen, ”Direct Methods for Transient Stability Analysis of Power Systems: Recent Results”, Proc. of the IEEE, vol. 73, no 12, pp 1703-1714, December 1985.

[11] C.L. DeMarco, “A Phase Transition Model for Cascading Network Failure”, IEEE Control Systems Magazine, vol. 21, no 6, pp 40-51, December 2001.

[12] Anthony N. Michel, A. A. Fouad, Vijay Vittal, “Power System Transient Stability Using Individual Machine Energy Functions”, IEEE Transactions on Circuits and Systems, vol. cas-30, No.5, May 1983.

[13] M. A. Pai, “Power System Stability”, 1981

[14] M. Vidyasagar, “Nonlinear Systems Analysis”, 2002

[15] A. R. Bergen, “Power System Analysis (2nd Edition)”,2000